Frontiers of Physics
https://doi.org/10.1007/s11467-021-1114-5
Front. Phys.
17(2), 23204 (2022)

TOPICAL REVIEW

Emerging of two-dimensional materials in novel memristor

Zhican Zhou[1,2,*], Fengyou Yang[2,*], Shu Wang[2,*], Lei Wang[2,3], Xiaofeng Wang[2], Cong Wang[4,†], Yong Xie[5,‡], Qian Liu[1,2,#]

[1] *MOE Key Laboratory of Weak-Light Nonlinear Photonics, Department of Physics, Nankai University, Tianjin 300071, China*
[2] *CAS Center for Excellence in Nanoscience, National Center for Nanoscience and Technology, University of Chinese Academy of Sciences, Beijing 100190, China*
[3] *College of Mathematics and Physics, Shandong Advanced Optoelectronic Materials and Technologies Engineering Laboratory, Qingdao University of Science and Technology, Qingdao 266061, China*
[4] *College of Mathematics and Physics, Beijing University of Chemical Technology, Beijing 100029, China*
[5] *School of Physics, Beihang University, Beijing 100191, China*
Corresponding authors. E-mail: [†] *wangcongphysics@mail.buct.edu.cn,* [‡] *xiey@buaa.edu.cn,* [#] *liuq@nanoctr.cn*
Received July 13, 2021; accepted August 26, 2021

The rapid development of big-data analytics (BDA), internet of things (IoT) and artificial intelligent Technology (AI) demand outstanding electronic devices and systems with faster processing speed, lower power consumption, and smarter computer architecture. Memristor, as a promising Non-Volatile Memory (NVM) device, can effectively mimic biological synapse, and has been widely studied in recent years. The appearance and development of two-dimensional materials (2D material) accelerate and boost the progress of memristor systems owing to a bunch of the particularity of 2D material compared to conventional transition metal oxides (TMOs), therefore, 2D material-based memristors are called as new-generation intelligent memristors. In this review, the memristive (resistive switching) phenomena and the development of new-generation memristors are demonstrated involving graphene (GR), transition-metal dichalcogenides (TMDs) and hexagonal boron nitride (*h*-BN) based memristors. Moreover, the related progress of memristive mechanisms is remarked.

Keywords memristor, resistive switching, 2D material, switching mechanism, conductive channel

Contents

1 Introduction

Since Strukov *et al.* [1, 2] in 2008 found the missing memristor conceived by Chua in 1971 [3], exploitation of non-volatile memory had drawn giant interests in computing science and multidiscipline on convinced that the traditional Von Neumann paradigm and integration architecture were facing its bottleneck and impending physical limits (∼ 5 nm) [4–8]. Conventional memristor has been used in the artificial chip to realize deep learning algorithms such as sparse coding [9, 10], reservoir computing [11], and used as an artificial nociceptor [12], which is a critical and special receptor of a sensory neuron to detect noxious stimulus. Yet it is noteworthy that the exact defination of memristor has sparked bitter controversy. Some researchers believe that it is inappropriate to use memristors as a replacement for all resisitive memory devices, and they consider that the property of pinched hysteresis loops alone cannot serve as a good indicator of memristors since that property is shared by some different types of devices [13, 14]. Besides, they also argued that for the real memristor, the functional dependence of its memory resistance on only the net charge (q), and this has not

* These authors contributed equally.
Special Topic: Graphene and other Two-Dimensional Materials (Eds. Daria Andreeva, Wencai Ren, Guangcun Shan & Kostya Novoselov).
This article can also be found at http://journal.hep.com.cn/fop/EN/10.1007/s11467-021-1114-5.

yet been demonstrated experimentally [13]. However, the controversy mentioned above is not the main content of this acticle, so we will not disscuss comprehensively about this. Here, we refer to a memoristor as a widely accepted defination, a device that depends on changes in resistance.

Memristor or resistive random access memory (RRAM) typically has the simple form of two terminals sandwiching a "switching" layer which enables stack readily in horizontal or vertical 3D framework, being accessible to ultra-high-density integration and low-cost fabrication [12, 15–17]. The emerging technologies have shown that the memristive (resistive switching, RS) device can be scaled to sub-10 nm feature sizes [18], and retains memory signals for years [15]. So far, the individual device has offered very appealing performance including nanosecond switching speed [19–21], trillion-cycles erase-write endurance [20, 22] and femtojoule energy consumption [23, 24]. The ultimate scaling of the RS layer or electrodes can be just few atom layers by integrated and tuned the properties of novel 2D materials [25, 26].

The typical RS effect involves ion redistribution in the solid-electrolyte layer. The working principle is focused generally on two sides: (i) valence change memory (VCM) [27] due to oxygen deficient (or oxygen-vacancy ionic-bridging) and cations migration [28]; (ii) electrochemical metallization (ECM) [29] owing to active metal cations drift from active nodes [30] to inert electrode. Besides, a thermochemical mechanism (TCM) [31] is also proposed and long-debated. A set/reset switching process includes generally the oxidation, migration, and reduction of the cation or anion species, leading to the formation/rupture of a conductive channel (e.g., conductive filament, CF) in the dielectric layer. The RS process can be abrupt (digital)/gradual (analog) based on the different responsive mechanisms evolving at different timescales, and also be unipolar/bipolar dependent on different internal ions diffusion processes. The devices in different RS types can realize various comuputing functions, for instance, the applications in neural networks [32–35], and boolean logic circuit [36–38].

In the past decade, graphene, transition-metal dichalcogenides (TMDs), and other non-carbon based material have been widely and thoroughly studied because of their novel physical phenomena and diversified applications ranging from nanoelectronics and nanophotonics to sensing and actuation at the nanoscale [25, 39, 40]. These burgeoning materials have also been used as the surface electrode or interlayer in the memristor or resistive switching device. Recently, Lu *et al.* and Liu *et al.* reported that graphene defect-engineering can be used to tune the size of the CF by controlling the oxygen vacancy and active metal ionic [41, 42]. In 2015, TMDs was first introduced into memristor, however, the memristive property was degraded due to unmanageable grain boundary types [43]. Later, the memristive phenomenon was discovered in a wide range of single layer TMDs (MoS_2, $MoSe_2$, WSe_2, and WS_2) [44, 45]. Guo and Wang *et al.* reported an atomically thin femtojoule memristive device, which only exhibits sub-nanometer filamentary switching with sub-pA operation current and femtojoule per bit energy consumption [46]. Based on the aggressive progress reported previously in this field, numerous reviews have been organized in the right past decade [6, 12, 15, 47]. In this review we will focus our concerns on mainly the memristive phenomena and development in new-generation memristors based on 2D layered material, and then remark the progress of memristive mechanism. Besides, we also summarise the methods of CF controlling in TMDs based memristor and conventional memristor, which may provide a feasible solution for ultimate application of the new-generation memristors.

We will organize this review as follows. Section 2 is about graphene and graphene oxide based memristors. Section 3 is about TMDs and other non-carbon based memristors. Section 4 is the discussion of the memristive mechanism in both 2D layered materials and conventional materials. At last, a brief summary and outlook of the new-generation memristor are presented.

2 Progress in new-generation intelligent memristors

2.1 Graphene and graphene oxide-based memristors

Graphene has attracted worldwide attention due to the fascinating properties predicted and measured, including stable monoatomic structure, super electron mobility, high thermal conductivity, unique mechanical properties, and the recently discovered superconductivity [48–52]. Recent years, a growing interest in memristive devices has also been directed toward graphene or graphene oxide-based memristors.

Even though graphene is generally not be used as the switching medium in memristive devices due to the super electron mobility, graphene and its other derivatives have been studied as electrodes and interfaces material due to their low manufacturing cost, high mechanical flexibility, and high optical transparency, which can practicley improve the device performances. Recently, A highly reliable, flexible memristor array consisting of graphene/Al_2O_3/MoS_2 heterostructures was built, where the graphene worked as a floating-gate, and 93% of the devices exhibit an on/off ratio of over $\times 10^3$ with an average ratio of 10^4 [53]. Halbritter *et al.* demonstrated that a SiO_x-based memristor was confined by few nanometer wide nanogaps between graphene electrodes, demonstrating that, the internal time scale, the dead time play a fundamental role in the system response to various driving signals except for the commonly observed bias voltage dependent set and reset times [54]. Graphene electrodes with organic resistive switching media provide high trans-

parency of 92%, holding long retention of 10^4 s and high I_{ON}/I_{OFF} of 10^6 [55]. As shown in Fig. 1(a), Choi *et al.* reported a good device performance with the endurance of 1.5×10^5 cycles, I_{ON}/I_{OFF} of 10^6 [56]. Even after bent over 1.5×10^5 times, switching characteristics change little. In 2020, Wang *et al.* reported that a cheap and mass-productive compacted self-assembly (CSA) graphene with hydrogen (H_2) plasma surface modification graphene was introduced into bottom electrode (BE) of gadolinium oxide (Gd_xO_y) memristors, realizing high rubustness and low operating voltages synapses in a single device [57]. As interface material, graphene is able to control interface oxygen ions channel, capture oxygen ions in memristive medium, and suppress surface effects [41, 42, 58]. In a standard memristor structure, the migration of oxygen ions is not well controlled leading to undesirably large leakage current, device-to-device and cycle-to-cycle variability issues, and device failure to reset. Graphene with controllable nanosized openings was inserted between Ta and Ta_2O_5 to modulate the oxygen ionic transport, redox reactions, and device performance. Working current was reduced by decreasing nanopore sizes. Therefore, lower energy consumption could be achieved at the same set/reset voltage [Fig. 1(b)] [41]. Liu *et al.* modulated the cation injecting path to the RS layer by structure-defective graphene to control the CF quantity and size [Fig. 1(c)] [42]. Finally, a low operating current ($\sim$ 1 μA) memory and a high driving current ($\sim$ 1 mA) selector are successfully realized in the same material system. Chaplygin *et al.* added graphene islands into a classic poly(ethylene oxide)/polyaniline (PEO/PANI) organic memristive device where the conductance of the PANI layer is regulated by the drifting of Li^+ ions [Fig. 1(d)] [58]. The graphene islands can capture the Li^+ ions in excess, thus failure of the device caused by PANI film reoxidation will be prevented. In other work, graphene was inserted into the device structure to suppress the surface effects such as chemisorption and surface band bending.

In contrast to graphene, graphene oxide (GO) sheets are oxygenated, loaded hydroxyl, epoxide functional groups, carbonyl, and carboxyl groups [59]. Electrical insulation originated from these functional groups allows GO to be a choice of switching medium for the memristive device. Two different mechanisms have been proposed to explain the unique electrical behavior: oxygen ion diffusion driven by the electric field and the formation of a metal filament due to the diffusion of the metal atom from the electrode under an electric field excitation. For the former mechanism, migration of oxygen ions makes the GO layer transform from sp^3 hybridized state to sp^2 state, corresponding high resistance state (HRS) to low resistance state (LRS) [60]. A metal–insulator–metal (MIM) structure where GO is in the middle of two Al electrodes is reported [61]. The presence of an aluminum oxide insulating film at the interface between the GO and Al electrode creates a contact resistance to participate in the switching process, while the GO layer just behaves as oxygen ions reservoir. In 2017, a novel bioinspired switching device was developed by stacking graphene oxide nanoribbon networks (GOR-Ns) into the layered GOR-N membrane (GOR-NM), with an excellent flexibility, reliability, and superior V_{ON}/V_{OFF} ratio of up to 10^6. The switching behavior was induced by the structural polarization of GOR-NM by asymmetric electrochemical oxidation/reduction creating oxygen concentration gradient [62]. Recently, Valov *et al.* presented that the moisture played a crucial role in the formation of oxygen vacancies, thus determining the forming voltage and kinetic process [63]. In addition to the oxygen ion drift, the formation of a metal filament within the insulating layer is another explanation of memristive behavior. This was clarified by a Cu/GO/Pt structure [64]. Applied a positive voltage to the top Cu electrode, metal ions migrates from the top electrode to the bottom electrode through the GO film. The resistance state switch from the HRS to the LRS when the filament reaches to the bottom electrode. An inversion of voltage causes back-diffusion of the metal ions. In 2021, Sahu *et al.* structured Ag/GO/fluorine-doped tin oxide memristor device, and this device sucessfully exhibits the essential synaptic learning behavior including analog memory characteristics, potentiation and depression [65].

2.2 TMDs and other non-carbon 2D layered material-based memristors

The graphene has been widely studied because of its rich physical and electronic properties. However, pristine graphene has not a bandgap, affecting its applications in some practical situations. TMDs with a general chemical formula of MX_2, where M is a transition metal atom (for example, Mo, W, Ti, Zr, Ta, Nb) and X is a chalcogen atom (for example, S, Se, Te), have the advantage over graphene by tunable bandgap, such as composition variations, thickness controlling and doping engineering.

To date, many types of RS device have been developed based on TMDs. In the beginning, TMDs are thought to be not ideally suited for memristors because of the intrinsic semiconductor property, they need to be functionalized to add an insulating layer. Liu *et al.* reported a flexible memory device with a stack of PET/RGO/MoS_2-PVP/Al fabricated by polymer-assisted exfoliation, and its I_{ON}/I_{OFF} ratio was only about 10^2 [66]. With the same device structure, Huang and Tan *et al.* had managed to mix MoS_2 with GO, P123, and ZIF-8 respectively. They found that the I_{ON}/I_{OFF} ratio of MoS_2 with ZIF-8 was enhanced to 7×10^4, and the RS property could remain about 1.5×10^3 s [67]. The memristive phenomenon had not been discovered in the pristine single-layer MoS_2 until Sangwan *et al.* reported a gate-tunable memristor, as shown in Fig. 2(a), based on grain boundary effects in single-layer MoS_2. The switching ratio was raised up to 10^3 and a dynamic negative differential resistance (NDR) was

found [43, 68]. However, The memristive characteristics of devices were strongly dependent on the grain boundary configurations, typically as parallel, perpendicular and intersecting configurations, and the set/reset processes need a higher voltage in the MoS_2 devices than the traditional memristors. Later, Cheng *et al.* reported a memristor based on only 1T phase MoS_2 with the structure of vertical Ag/1T-MoS_2/Ag, where an on/off ratio of three orders of magnitude, tiny set or reset voltage about 0.2 V and good cycle endurance above 1000 times were realized [Fig. 2(b)] [69]. In the reported devices, a memristive phenomenon occurred since the electrical field induced lattice distortion in 1T phase MoS_2, leading to the change of resistance. However, these devices were fabricated by spin-coating the MoS_2 nanoflakes on the active Ag electrode, this made it ambiguous whether only 1T phase MoS_2 play an essential role in the RS effects or mixing with other conductive mechanisms. For example, the active Ag electrodes form the conductive channels by the conventional redox processes. At the same time, Yoshida *et al.* reported that memristive behavior could occur within 2D 1T-TaS_2 crystals, and memristive characteristic depended on the thickness of the 2D crystals [70]. Although the RS mechanisms are still in dispute so far and single-layer TMDs based memristors have difficulties in preparing, the vertical MIM structure devices are of contemporary preference owing to their smaller footprint and denser integration not only from a fundamental research perspective but also practical application perspective.

Recently, Akinwande *et al.* made an remarkable progress, overturning the long-standing view that nonvolatile RS is not scalable to sub-nanometer due to the leakage current issues [Fig. 2(c)] [44]. They obtained observations of resistive switching phenomenon in a variety of single-layer TMDs atomic sheets (MoS_2, $MoSe_2$, WS_2, and WSe_2) in the advantageous MIM configurations [45]. In these memristors, an on/off ratio above 10^4 was achieved, and the storage state remained above 10^6 s. Then Combining the scanning tunneling microscopy/scanning tunneling spectroscopy (STM/STS) and local transport studies, they took memristor based on monolayer MoS_2 as example, built a model named dissociation–diffusion–adsorption (DDA), and elucidated the origin of the switching mechanism in atomistic level [71]. Involving the intelligent TMDs-based memristors, one of the most important questions is the robustness in the use of an array of memristors. In March 2018, Miao *et al.* proposed a strategy to enhance the robustness based on a van der Waals heterostructure made of fully layered 2D materials (graphene/$MoS_{2-x}O_x$/graphene) [Fig. 2(d)], in which repeatable bipolar resistive switching with endurance up to 10^7 and high thermal stability with an operating temperature of 340 °C were exhibited [72]. In situ STEM was performed to reveal the nature of the robustness and the

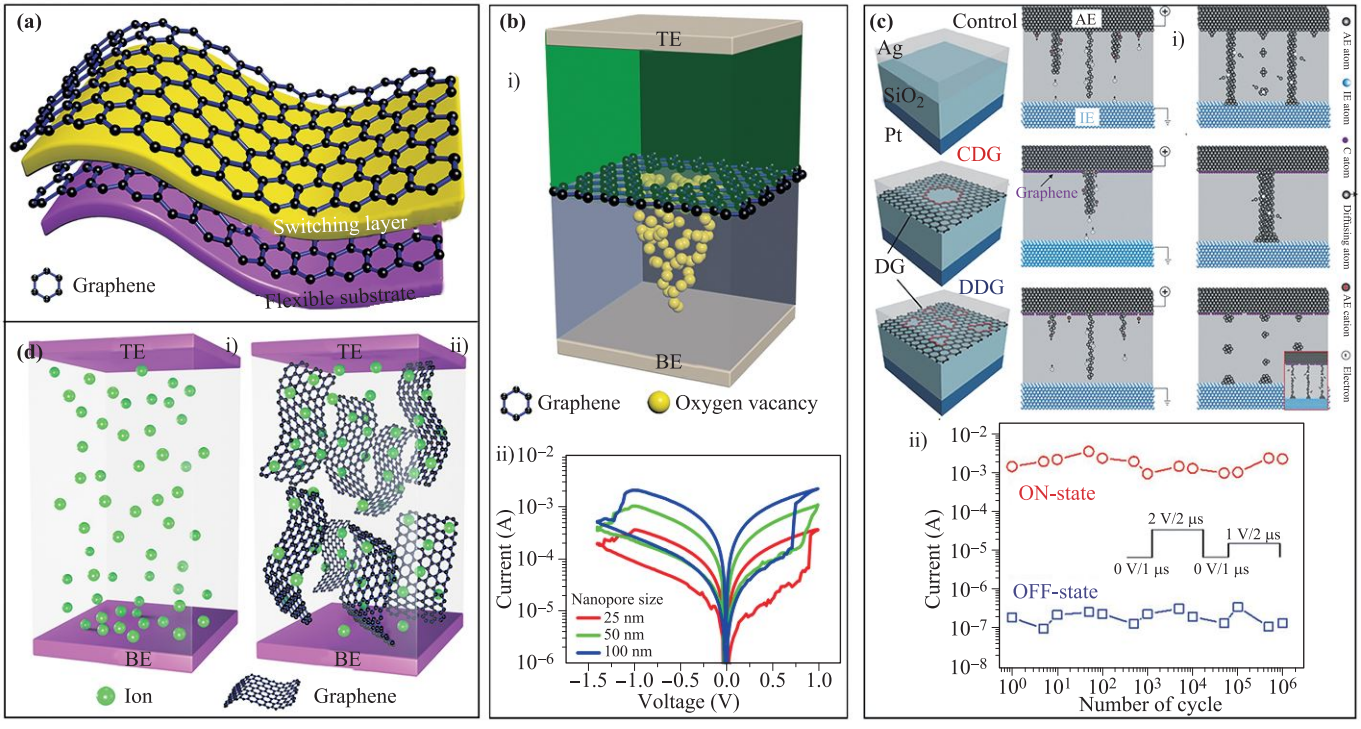

Fig. 1 **(a)** Flexible organic bistable devices based on graphene embedded in an insulating poly(methylmethacrylate) layer, being able to bend over 1.5×10^5 times. **(b)** Tuning ionic transport in memristive devices by graphene with engineered nanopores. Reproduced from Ref. [41], Copyright © 2016 American Chemical Society. **(c)** Cell structure and schematic illustrations of the cation migration by graphene-based defects-engineering. Reproduced from Ref. [42], Copyright © 2018 WILEY-VCH Verlag GmbH & Co. KGaA, Weinheim. **(d)** The drifting of the Li^+ ions based on thin polyanilinegraphene films.

related RS mechanism. They indicated that the extra-high thermal stability of the $MoS_{2-x}O_x$ layer could effectively avoid the undesirable migration of oxygen and sulfur ions, and prevent possible reactions between the conduction channels and the surrounding media. Guo *et al.* also reported a n-MoS_2/p-Si heterostructure with photonic potentiation, and the electric habituation was used as memristive synapses [73]. Versatile synaptic neuromorphic functions, such as short-term memory, long-term memory, and paired-pulse facilitation, were successfully mimicked in their memristor system. Chen *et al.* reported an artificial flexible visual memory system based on an UV-motivated memristor [74]. This memory system can realize the detection of UV light distribution with a patterned image and the memory information can keep for a long retention time. Although the performance of the TMDs-based memristor was improved rapidly, the key parameters (such as switching speed and retention time) are thought to be still far from their traditional counterparts.

Hexagonal boron nitride (*h*-BN), which is a 2D layered insulator material, sometimes referred as "white graphene". Compared to the traditional dielectrics like SiO_2 or TMOs, *h*-BN can be prepared with a very flat/uniform surface that may reduce variations of the memristor devices. Its superior chemical stability can inhibit interaction with adjacent layers, and its high thermal conductivity may favor heat dissipation in the electronic devices. On the other hand, compared to other 2D conductive and semiconducting materials, *h*-BN do not need any transfer process to build the memristor devices, as it can be grown directly on a metallic substrate (act as top/bottom electrode) using chemical vapor deposition (CVD) technique, and the insulating nature of *h*-BN can result in a large current on/off ratio.

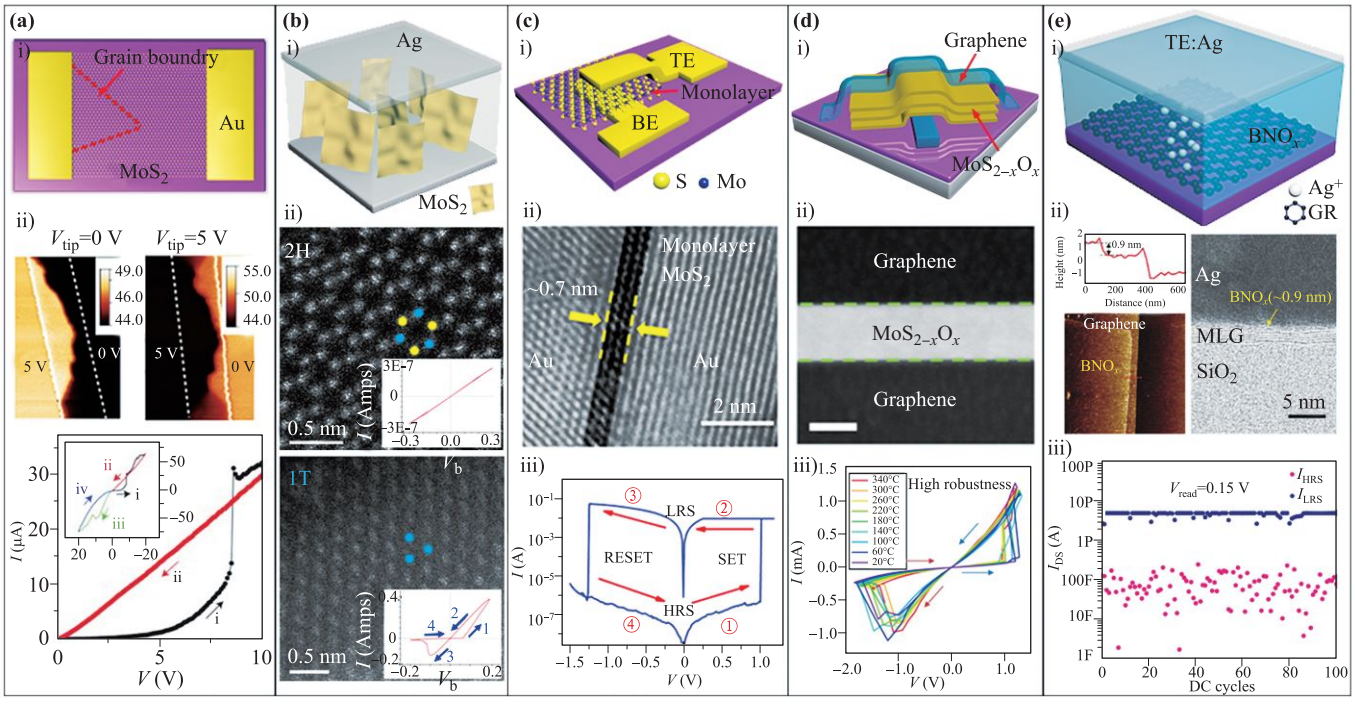

Fig. 2 **(a)** Gate-tunable memristor based on boundaries in monolayer MoS_2. i) The device structure of gate-tunable memristor based on the motion of S vacancies. ii) The grain boundary drifting under the set voltage from 0 V to 5 V and the memristive characteristic with switching ratio up to 10^3. Reproduced by Ref. [43], Copyright © 2015 Springer Nature. **(b)** An ideal memristor based on 1T phase MoS_2. i) The device structure of vertical Ag/1T-MoS_2/Ag memristor. ii) The TEM images and electric properties of 2H phase MoS_2 and 1T phase MoS_2. Reproduced from Ref. [69], Copyright © 2016 American Chemical Society. **(c)** Atomristor based on single-layer transition-metal dichalcogenides atomic sheets. i) The schematic device structure. ii) The TEM image of the Au/MoS_2/Au memristor (thickness ~0.7 nm). iii) The memristive feature of MoS_2 based memristor with $I_{ON}/I_{OFF} > 10^4$. Reproduced from Refs. [44, 45], Copyright © 2018 American Chemical Society, Copyright © 2020 Wiley-VCH GmbH. **(d)** Robust memristors based on layered twodimensional materials. i) The MoS_2 based memristor with a structure of graphene/MoS_2/graphene. ii) Clear interface in the memristor between the MoS_2 interlayer and graphene electrode. iii) The high thermal stability under different operating temperatures up to 340 °C. Reproduced from Ref. [72], Copyright © 2018 Springer Nature. **(e)** Atomically thin femtojoule memristive device based on monolayer BNO_x. i) Monolayer BNO_x based memristor with the structure of Ag/BNO_x/Graphene. ii) AFM and TEM images of the BNO_x and memristor device, respectively (thickness ~ 0.9 nm). iii) The changes of high/low resistive states of the memristor under a sub-pA operation current with endurance up to 100 cycle times. Reproduced from Ref. [46], Copyright © 2017 WILEY-VCH Verlag GmbH & Co. KGaA, Weinheim.

Over the last decade, memory devices based on hybrid nanocomposites including polymers and *h*-BN is developed owing to their capacity of trapping charged carriers to realize the nonvolatile memory effect. Lee *et al.* reported a novel flexible memristor device comprising an ultrathin *h*BN ($h \sim 3$ nm) active layer sandwiched between the Ag top electrode and Cu foil bottom electrode on a polyethylene terephthalate substrate [70]. The as-fabricated Ag/*h*-BN/Cu foil memory device showed excellent performance in various aspects including on/off ratio (~ 100), write/erase cycling (~ 550), retention time ($\sim 3\times10^3$ s) and bending endurance (~ 750 cycles). Soon after, Choi *et al.* reported that a flexible resistive memory device based on a stack of *h*-BN/polymers nanocomposites (polyvinyl alcohol) [75]. The on/off ratio at a read voltage of 0.26 V was recorded to 4.8×10^2, which is enough to distinguish the HRS from the LRS. The memristors also possessed good mechanical robustness over 1500 cycles bending. Lanza *et al.* repored that the coexistence of forming free bipolar and threshold-type RS was existed in mutilayer BN reactorand and developed a series of worthwhile RRAM devices with low operation voltages down to 0.4 V, high current on/off ratio up to 10^6, and long retention time above 10 h, as well as low variability [76]. They also achieve good control of the device properties by tuning the thickness and grain size of the *h*-BN stack, as well as by inserting interfacial graphene electrodes. As far as we know, the morphology and dimension of CF formed in a memristive device are strongly influenced by the thickness of its switching medium layer. Appropriate scaling of this active layer thickness is critical toward reducing the operating current, voltage, and energy consumption in filamentary-type memristors. Guo and Wang *et al.* reported an atomically thin femtojoule memristive device, which only exhibits sub-nanometer filamentary switching with sub-pA operation current and femtojoule per bit energy consumption [Fig. 2(e)] [46]. This device has a stack of Ag/BNO_x/Graphene, where a very interesting feature is the strong dependence of its switching characteristics on the thickness of the BNO_x layer. Devices with a thinner BNO_x layer can be operated reliably under the lower current and voltage in both the set and reset states. It is worth noting that the formation/rupture of CFs in a sub-nanometer thickness of *h*-BN is reported in the first time, three months later than the related reports of MoS_2 in a sub-nanometer thickness [44, 46].

In addition, Akinwande *et al.* reported the nonvolatile RS (NVRS) capabilities of single-layer BN grown by chemical vapor deposition (CVD) vertically in a MIM sandwich configures [77]. The devices they fabricated in both bipolar and unipolar modes could achieve fast switching speeds (15 ns) and high switching ratio (10^7) via pulse manipulation. The fabrication of this single-atom *h*-BN NVRS device extended the atomic resistance member to a 2D insulator, which could yield newer applications in printing electronics, ultrathin flexible memory, radio-frequency switches, and neuromorphic computing. Very recently in 2020, Chen *et al.* have sucessfully fabricated high-density memristive crossbar arrays based on wafer scale 2D *h*-BN with a high yield of 98%, and used to model an artificial neural network for image recognition [78], which have paved the way for the mature applications in the future industry.

2.3 Performance index analysis

A statistical analysis of performance index in new-generation memristors is performed in order to compare the existing data visually and promote the index renewal in the memristors. Figure 3 shows the related data according to 45 recent reports collected since 2015. (Details see Table 1). In these references, the highest I_{ON}/I_{OFF}, cycle times and retention time are 10^{10} [44], 10^7 times [51] and 10^6 s [72] respectively. Among them, the values of I_{ON}/I_{OFF} and cycle times may meet the demand in the development of RRAM or memristor devices, but the retention time is still not satisfactory. Some data in Fig. 3 were located in the yellow area of the axes, meaning that few memristors possessed comprehensive and excellent performance index including differentiable I_{ON}/I_{OFF}, high cycle times and long retention time. Secondly, some graphene-based memristors marked by red stars exhibit preferable performance compared to TMDs, BN, and BP based memristors, which was mainly attributed to the favorable combination of conventional TMOs. Thirdly, most research articles paid much attention to I_{ON}/I_{OFF}, cycle times and retention time. The faster programming/erasing speed, longer retention time and lower operating voltage, which

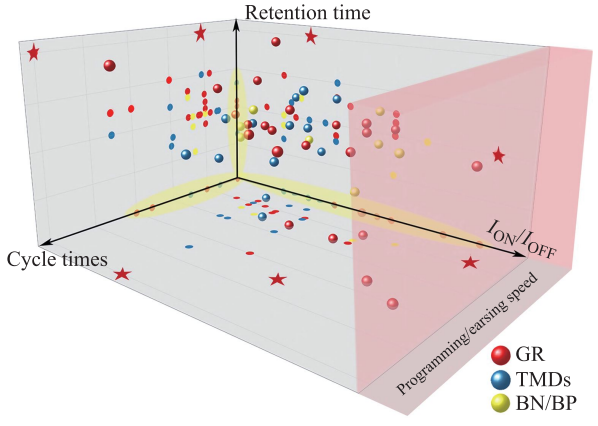

Fig. 3 Device performance indexes of memristors based on Graphene/Graphene oxides (Red balls and their projection), TMDs (Blue balls and corresponding projection), BN/BP (Yellow balls and corresponding projection) along three axes, I_{ON}/I_{OFF}, Cycle times and Retention time respectively. The red star on the projective plane implies the best value obtained according to our statistics. Data in the yellow regions on the axis represent only one or two parameters provided in the references.

Table 1 Performance indexes in 45 articles since 2015.

Ref.	Structure	I_{ON}/I_{OFF}	Cycle times	Retention time (s)
[46]	Ag/BNO_x/Gr	10^7	> 100	10^4
[68]	Au/monolayer-MoS_2-GB/Au	10^2	15	
[69]	Ag/1T-MoS_2/Ag	10^3	10^3	
	Au/SL-MoS_2 /Au	10^4	150	> 10^6
[44]	$MoSe_2$	10^7		> 10^4
	WS_2	10^{10}		> 10^6
[72]	GR/$MoS_{2-x}O_x$/GR	10^4	10^7	> 10^5
[73]	n-MoS_2/p-Si	4×10^3	15	150
[74]	Ni/Al_2O_3/Au	10^2	> 50	> 1600
[75]	Ag/*h*-BN-polymers nanocomposites /ITO	4.8×10^2	10^3	
[76]	Ti/MLG/thin *h*-BN/MLG/Au	10^6	> 450	4×10^4
[53]	Gr/Al_2O_3/MoS_2	10^4	8000	
[54]	Gr/SiO_x/Gr	> 10^4	> 1000	
[55]	ZnO–GQDs	10^6	10^2	10^4
[56]	Al/PMMA/MLG/PMMA/ITO	4.4×10^6	1.5×10^5	10^5
[42]	Ag/DG/SiO_2/Pt	5×10^8	10^6	10^4
[62]	GOR-NM	10^6	> 1000	10^6
[79]	PCBM−MoS_2	3×10^2		> 10^4
[80]	Ag/Gd_xO_y/Al_xO_y/TLG/Ir	10^3	250	10^4
[81]	Al/GO-TiO_2/ITO/PET	10^2	10^4	> 10^5
[82]	Sb_2Te_3 nanosheets	10^3	20	
[83]	metal/GO(T)/metal	10^4		
[84]	Cu/ZnS/Gr/Cu	10^6	110	3000
[85]	Au/Ni/FeO_x–GO/Si_3N_4/n^+-Si	> 10^4	100	5 hours
	Cu/GO/Pt	20	> 100	> 10^4
[86]	Ag TE/*h*-BN/Cu foil	100	550	3×10^3
	Al/BP film/ITO	3×10^5	–	> 10^5
[87]	Cu/nanohole-Gr/HfO_2/Pt	10^6	10^7	2×10^5
[88]	PEDOT:PSS/(GO)/m-PEDOT:PSS	10^4	1000	
[89]	graphene/$SrTiO_3$/Nb:$SrTiO_3$	10^3	150	
[90]	Gr/*h*-BN/Gr	10^3	50	
[91]	GO-ZnONRs	3.3×10^5	1000	5×10^4
[92]	Al/1T@2H-MoS_2-PVPITO/ PET	2×10^2	10^4	600
[93]	Pt/GO/Ti/Pt	10^2	10^4	10^5
[94]	Au/MoS_2-PVK/ITO	3×10^4	10^6	
[95]	MoS_2/$BaTiO_3$/$SrRuO_3$	10^4		48 hours
[96]	Al/GQD: poly(methyl silsesquioxane)/ITO	10^6		2×10^4
[97]	Au/[N-GO(+)/GO(–)]$_n$/Al/PES	10^9	50	10^4
[98]	GO/MoS_2/GO	100	> 10^2	> 10^4
[99]	Ag/*h*-BN/Cu/PET	100	550	3×10^3
[100]	Al/BP film/ITO	3×10^5		10^5
[101]	Al/AlO_x/GR/SiO_2	10^5		
[43]	Ta/G/TaO_x/Pt	10^6	100	
[102]	Al/GOZNS/ITOPET	100	200	10^4
[103]	graphene/AlO_x/TiO_x/ITO	> 300	100	10^4
[104]	Au/Al_2O_3/BP/Al_2O_3/BP	10^3		1000
[105]	Ga-doped ZnO/MX_2–PVA/Ag	3×10^3		350

are very important to the development of RRAM and AI chips, have not receive enough attention. In principle, all of these will be enhanced by introducing 2D materials. However, restricted by the fabrication process, current 2D materials facing several unavoidable shortages such as Van der Waals gap and Fermi pining which will tremendously harm the performances of the devices by inducing barriers and gap states to the system. Therefore, compared to conventional TMOs memristors, there is still a huge room for development of the new-generation memristors based on 2D materials. Besides, RS mechanisms need also be clarified clearly. Subsequently, we will give insights based on our knowledge in this review.

3 Memristive mechanisms of new-generation intelligent memristors

The common RS mechanisms are divided into two categories: that is the aforementioned ECM and VCM. The essence of the switching mechanisms is subject to the ionic migration and reconfiguration processes, which lead to the formation/rupture of conductive channels in the dielectric layer [5–7, 16, 17]. Besides the conventional three layers structure consisting of active electrode/switching-layer/inert electrode, 2D materials are also intensively investigated as an interfacial layer between the electrode and the interlayer, or within the interlayer. The goal of the addition of 2D materials is to improve the variation issue and performance of memristors by controlling the formation of conductive channels or charge tunneling/trapping processes utilizing the impermeability and high work-function of graphene and similar 2D materials. Nevertheless, the RS mechanisms are much the same in most of the devices as the ECM and VCM mentioned. Specifically, the ECM memory includes generally six evolving processes, as shown schematically in Fig. 4(a). First, the active metal electrode (e.g., Ag or Cu) is ionized into cations under an external voltage as shown in the former two panels. With the increase of the applied bias, the rate of ionization is speeded up given by the Butler–Volmer equation [106]. Affected by the applied electric field, the cations diffuse toward the inert electrode through the solid electrolyte gradually. An inverted-cone cation distribution can be formed due to the diffusion gradient generated with time, as shown in panel three. Subsequently, the cations are reduced to metal atoms from the beginning contact of the inert electrode and develop toward the active electrode. Finally, an upright-cone CF can be created owing to the reduction and cation migration as shown in panel four and five. A related set and LRS is established in the RS devices. As the polarity of the voltage is switched, resistance hot-spot effect (as shown in panel five top-center) and facilitated atom diffusion at the narrowest segment of the CF result in the fast fusing process referring to Ohm's law (power $\propto$ resistance $\propto$ 1/area). Decomposition and reversed diffusion make the CF degenerate into the active electrode, leading to the reset (HRS) process of the device as shown in panel five and six.

The VCM processes in traditional materials are related to the oxygen-vacancy ionic-bridging and decomposition processes. Figure 4(b) expressed a VCM process existed in MoS_2 based memristors. In the first set process, the thermophoresis effect due to the Joule heating drives S atoms away from the channel region and left the S vacancies forming the CF, leading to the ON state as shown in panels one and two. In the reset process, the oxygen atoms move into the channel region and occupy the sites of S vacancies so as to recover back to the initial OFF state as shown in panels three and four. It should be noted that the filled oxygen ions here are more movable than the sulfur ions due to the lower motion barrier. During the next set/reset process, the oxygen ions would be driven out/in of the channel region and play a major role in the RS processes due to the prominent thermophoresis effect and the steep temperature gradient produced by Joule heating. This VCM mechanism has been verified by in situ STEM [67].

As numerous reviews have already mentioned, controlling of the CF formation is very important to address the variation issue in practical applications of an array of memristor devices. Here, we also summarize the latest progress in controlling strategies of the CF formation both in employing the conventional RS materials with innovative designs [Figs. 4(c)–(e)] and new-generation 2D layered materials [Fig. 2(c)]. Figure 4(c) demonstrates a design strategy that uniformity of device performance can be improved by using engineered electrodes with protrusions or wedge shapes [30]. Choi and colleagues had presented a similar approach by grown SiGe materials epitaxially with vertically aligned high-density threading dislocations. The CF was observed to form preferentially along the dislocations [29]. But an evident drawback of the approach is the high temperature for SiGe growth, which would be incompatible with the existing integration technologies [20]. Figure 4(d) describes that a Ta interfacial layer is important in forming an enriched oxygen reservoir, which facilitates the oxygen diffusion in the dielectric layer. Compared with metal Ta, a metal Ti layer forms rough granular structure at the electrode/Ti interfaces, which limit oxygen scavenging and diffusibility [107]. But, it could be an effective strategy to control the ionic bridging between the electrodes by this kind of intercalating methods. Another interesting design of the conductive pathway is the use of mesopores materials, such as Silica mesopores [108]. The orientation of mesopores in the dielectric silica layer had been demonstrated to modulate the short-term plasticity of an artificial memristive synapse as in Fig. 4(e). The fastest current increase was implemented by successive voltage pulses with vertical mesopores orientation. Besides, the concept of metaplasticity has been introduced to mediate the CF variations in memristors [109]. A prim-

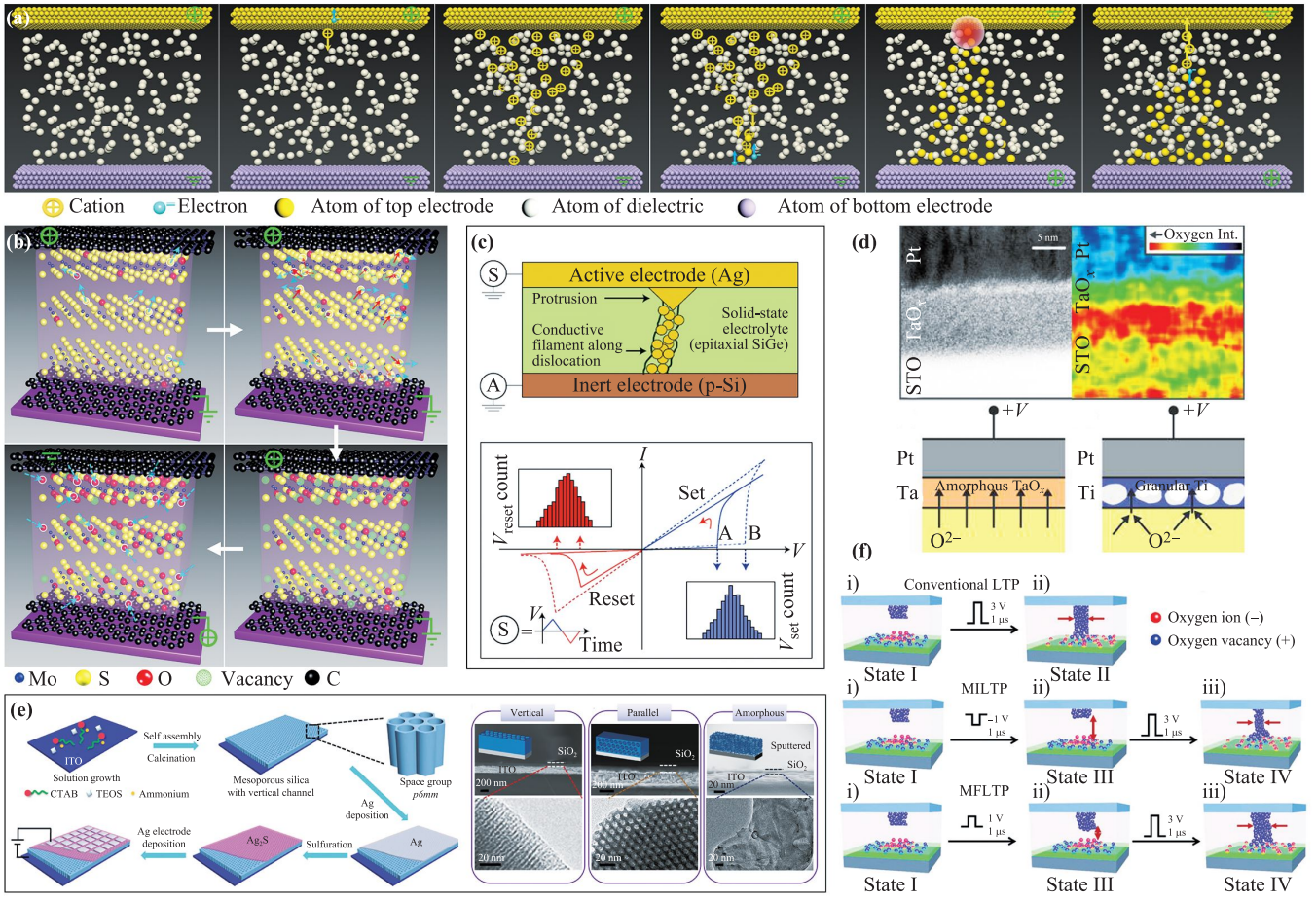

Fig. 4 **(a)** The electrochemical metallization mechanism involved in the 2D materials based memristors, where the set and reset processes are demonstrated by schematic panels from left to right. In panel five, the red region represents the hot-spot area generated by Joule heating, which would break down the formed conductive filament and result in the reset process. **(b)** The valence change memory mechanism existed in MoS_2 based memristors, where the set and reset processes are dominated by diffusion and migration of sulfur ions, the exchange between sulfur ions and oxygen ions, and diffusion and migration of oxygen ions. **(c)** Conductive-bridge memristors with an engineered protrusion and typical I–V hysteretic curve. Reproduced from Ref. [30], Copyright © 2018 Springer Nature. **(d)** STEM image (left panel) and the EDX mapping of oxygen K-line intensity (right panel) at the Pt/Ta/STO interface after the gradual resistance decrease. The bottom panels illustrated schematically the oxygen scavenging processes in the uniform Ta layer and granular Ti interlayer. Reproduced from Ref. [107], Copyright © 2018 American Chemical Society. **(e)** The schematic fabricated procedure of the memristive synapse with vertical multiporous silica and SEM and TEM images of the cross-section for the memristors. Reproduced from Ref. [108], Copyright © 2018 WILEY-VCH Verlag GmbH & Co. KGaA, Weinheim. **(f)** The schematic diagrams showing the variation of the shape of the conducting filament in various states. Reproduced from Ref. [109], Copyright © 2018 The Royal Society of Chemistry.

ing stimulus is essential to affect the formation of CF and its shapes as shown in Fig. 4(f). In addition, graphene and similar 2D materials have also been demonstrated to control the CF stability by using, e.g., defect engineering, as we have mentioned in Fig. 1(c) [42].

4 Outlook for new-generation intelligent memristors

Diverse achievements have been made in the current research of new generation intelligent memristors, such as atomristors based on TMDs, atomically thin femtojoule memristive device based on BNO_x and memristor with excellent robustness based on the 2D layered material. However, the practical applications of the memristor or RRAM are facing several challenges, including cycling endurance being still much smaller than that of conventional volatile memories and the large device-to-device (spatial) and cycle-to-cycle (temporal) variations. The high quality and large-area 2D materials are still urgently needed for developing robust memristor or resistive switching systems. In addition, conventional memristor has been used in the artificial chip to realize deep learning algorithms

such as sparse coding, reservoir computing, and as true random number generator to generates a string of random bits, which can be used as a cryptographic key. The performance of the logical operation, matrix multiplication and other relative modules based on new-generation intelligent memristor still need to be investigated continuously and in depth.

Although there is a long way to reach the ultimate applications and industrialization, we deeply believe that memristor is still the most promising candidates not only for the next generation of highly scalable memory devices and neuromorphic computing paradigm, but also for being building units for other widespread applications such as cryptography, LED display, synergetic enhancement with magnetic switching, and compute-in-memory concepts for big-data analysis and Internet of Things tasks.

Acknowledgements This work was supported by the National Natural Science Foundation of China (NSFC) (Nos. 51971070 and 10974037), National Key Research Program of China (No. 2016YFA0200403), Eu-FP7 Project (No. 247644), CAS Strategy Pilot Program (No. XDA 09020300). C. Wang acknowledges the support of the Fundamental Research Funds for the Central Universities (buctrc 202122). Y. Xie acknowledges the support of Beihang Youth Talent Funding Plan (No. YWF-18-BJ-Y-196).

References

1. D. B. Strukov, G. S. Snider, D. R. Stewart, and R. S. Williams, The missing memristor found, *Nature* 453 (7191), 80 (2008)
2. J. J. Yang, M. D. Pickett, X. Li, D. A. Ohlberg, D. R. Stewart, and R. S. Williams, Memristive switching mechanism for metal/oxide/metal nanodevices, *Nat. Nanotechnol.* 3(7), 429 (2008)
3. L. Chua, Memristor — The missing circuit element, *IEEE Trans. Circuit Theory* 18(5), 507 (1971)
4. Y. Yang and W. Lu, Nanoscale resistive switching devices: Mechanisms and modeling, *Nanoscale* 5(21), 10076 (2013)
5. D. Ielmini, Resistive switching memories based on metal oxides: Mechanisms, reliability and scaling, *Semicond. Sci. Technol.* 31(6), 063002 (2016)
6. F. Hui, E. Grustan-Gutierrez, S. Long, Q. Liu, A. K. Ott, A. C. Ferrari, and M. Lanza, Graphene and related materials for resistive random access memories, *Adv. Electron. Mater.* 3(8), 1600195 (2017)
7. J. Lee and W. D. Lu, On-demand reconfiguration of nanomaterials: When electronics meets ionics, *Adv. Mater.* 30(1), 1702770 (2018)
8. T. Zanotti, F. M. Puglisi, and P. Pavan, Smart logic-in-memory architecture for low-power non-Von Neumann computing, *IEEE J. Electron. Dev. Soc.* 8, 757 (2020)
9. P. M. Sheridan, F. Cai, C. Du, W. Ma, Z. Zhang, and W. D. Lu, Sparse coding with memristor networks, *Nat. Nanotechnol.* 12(8), 784 (2017)
10. D. H. Lim, S. Wu, R. Zhao, J. H. Lee, H. Jeong, and L. Shi, Spontaneous sparse learning for PCM-based memristor neural networks, *Nat. Commun.* 12, 319 (2021)
11. C. Du, F. Cai, M. A. Zidan, W. Ma, S. H. Lee, and W. D. Lu, Reservoir computing using dynamic memristors for temporal information processing, *Nat. Commun.* 8, 2204 (2017)
12. J. H. Yoon, Z. Wang, K. M. Kim, H. Wu, V. Ravichandran, Q. Xia, C. S. Hwang, and J. J. Yang, An artificial nociceptor based on a diffusive memristor, *Nat. Commun.* 9(1), 417 (2018)
13. J. Kim, Y. V. Pershin, M. Yin, T. Datta, and M. Di Ventra, An experimental proof that resistance-switching memory cells are not memristors, *Adv. Electron. Mater.* 6(7), 2000010 (2020)
14. Y. V. Pershin and M. Di Ventra, A simple test for ideal memristors, *J. Phys. D Appl. Phys.* 52(1), 01LT01 (2018)
15. J. J. Yang, D. B. Strukov, and D. R. Stewart, Memristive devices for computing, *Nat. Nanotechnol.* 8(1), 13 (2013)
16. Z. Wang, M. Rao, R. Midya, S. Joshi, H. Jiang, P. Lin, W. Song, S. Asapu, Y. Zhuo, C. Li, H. Wu, Q. Xia, and J. J. Yang, Threshold switching of Ag or Cu in dielectrics: Materials, mechanism, and applications, *Adv. Funct. Mater.* 28(6), 1704862 (2018)
17. M. A. Zidan, J. P. Strachan, and W. D. Lu, The future of electronics based on memristive systems, *Nat. Electron.* 1(1), 22 (2018)
18. B. Govoreanu, G. Kar, Y. Chen, V. Paraschiv, et al., 10 nm×10 nm Hf/HfO_x crossbar resistive RAM with excellent performance, reliability and low-energy operation, 2011 International Electron Devices Meeting, IEEE, p. 31.6.1 (2011)
19. A. C. Torrezan, J. P. Strachan, G. Medeiros-Ribeiro, and R. S. Williams, Sub-nanosecond switching of a tantalum oxide memristor, *Nanotechnology* 22(48), 485203 (2011)
20. S. Goswami, A. J. Matula, S. P. Rath, S. Hedström, S. Saha, M. Annamalai, D. Sengupta, A. Patra, S. Ghosh, H. Jani, S. Sarkar, M. R. Motapothula, C. A. Nijhuis, J. Martin, S. Goswami, V. S. Batista, and T. Venkatesan, Robust resistive memory devices using solution-processable metal-coordinated azo aromatics, *Nat. Mater.* 16(12), 1216 (2017)
21. A. M. Mostafa and A. A. Menazea, Laser-assisted for preparation ZnO/CdO thin film prepared by pulsed laser deposition for catalytic degradation, *Radiat. Phys. Chem.* 176, 109020 (2020)
22. K. H. Kim, S. Hyun Jo, S. Gaba, and W. Lu, Nanoscale resistive memory with intrinsic diode characteristics and long endurance, *Appl. Phys. Lett.* 96(5), 053106 (2010)
23. X. Feng, Y. Li, L. Wang, S. Chen, Z. G. Yu, W. C. Tan, N. Macadam, G. Hu, L. Huang, L. Chen, X. Gong, D. Chi, T. Hasan, A. V. Y. Thean, Y. W. Zhang, and K. W. Ang, A fully printed flexible MoS_2 memristive artificial synapse with femtojoule switching energy, *Adv. Electron. Mater.* 5(12), 1900740 (2019)

24. X. Yan, Q. Zhao, A. P. Chen, J. Zhao, Z. Zhou, J. Wang, H. Wang, L. Zhang, X. Li, Z. Xiao, K. Wang, C. Qin, G. Wang, Y. Pei, H. Li, D. Ren, J. Chen, and Q. Liu, Vacancy-induced synaptic behavior in 2D WS_2 nanosheet–based memristor for low-power neuromorphic computing, *Small* 15(24), 1901423 (2019)
25. B. Radisavljevic, A. Radenovic, J. Brivio, V. Giacometti, and A. Kis, Single-layer MoS_2 transistors, *Nat. Nanotechnol.* 6(3), 147 (2011)
26. J. Jiang and Z. Ni, Defect engineering in two-dimensional materials, *J. Semicond.* 40(7), 070403 (2019)
27. A. Sawa, Resistive switching in transition metal oxides, *Mater. Today* 11(6), 28 (2008)
28. A. Wedig, M. Luebben, D. Y. Cho, M. Moors, K. Skaja, V. Rana, T. Hasegawa, K. K. Adepalli, B. Yildiz, R. Waser, and I. Valov, Nanoscale cation motion in TaO_x, HfO_x and TiO_x memristive systems, *Nat. Nanotechnol.* 11(1), 67 (2016)
29. S. Choi, S. H. Tan, Z. Li, Y. Kim, C. Choi, P. Y. Chen, H. Yeon, S. Yu, and J. Kim, SiGe epitaxial memory for neuromorphic computing with reproducible high performance based on engineered dislocations, *Nat. Mater.* 17(4), 335 (2018)
30. D. B. Strukov, Tightening grip, *Nat. Mater.* 17(4), 293 (2018)
31. D. Ielmini, R. Bruchhaus, and R. Waser, Thermochemical resistive switching: Materials, mechanisms, and scaling projections, *Phase Transit.* 84(7), 570 (2011)
32. Y. Zhang, X. Wang, and E. G. Friedman, Memristor-based circuit design for multilayer neural networks, *IEEE Trans. Circuits Syst. I Regul. Pap.* 65(2), 677 (2017)
33. P. Wijesinghe, A. Ankit, A. Sengupta, and K. Roy, An all-memristor deep spiking neural computing system: A step toward realizing the low-power stochastic brain, *IEEE Transactions on Emerging Topics in Computational Intelligence* 2(5), 345 (2018)
34. T. Kim, S. Hu, J. Kim, J. Y. Kwak, J. Park, S. Lee, I. Kim, J. K. Park, and Y. J. Jeong, Spiking neural network (SNN) with memristor synapses having non-linear weight update, *Front. Comput. Neurosci.* 15, 22 (2021)
35. A. S. Sokolov, H. Abbas, Y. Abbas, and C. Choi, Towards engineering in memristors for emerging memory and neuromorphic computing: A review, *J. Semicond.* 42(1), 013101 (2021)
36. L. Xie, H. A. Du Nguyen, M. Taouil, S. Hamdioui, et al., Fast boolean logic mapped on memristor crossbar, 2015 33rd IEEE International Conference on Computer Design (ICCD), IEEE, p. 335 (2015)
37. H. Tan, G. Liu, H. Yang, X. Yi, L. Pan, J. Shang, S. Long, M. Liu, Y. Wu, and R. W. Li, Light-gated memristor with integrated logic and memory functions, *ACS Nano* 11(11), 11298 (2017)
38. L. Xu, R. Yuan, Z. Zhu, K. Liu, Z. Jing, Y. Cai, Y. Wang, Y. Yang, and R. Huang, Memristor-based efficient in-memory logic for cryptologic and arithmetic applications, *Adv. Mater. Technol.* 4(7), 1900212 (2019)
39. S. Hussain, K. Xu, S. Ye, L. Lei, X. Liu, R. Xu, L. Xie, and Z. Cheng, Local electrical characterization of two-dimensional materials with functional atomic force microscopy, *Front. Phys.* 14(3), 33401 (2019)
40. L. Meng, Y. Ma, K. Si, S. Xu, J. Wang, and Y. Gong, Recent advances of phase engineering in group VI transition metal dichalcogenides, *Tungsten* 1(1), 46 (2019)
41. J. Lee, C. Du, K. Sun, E. Kioupakis, and W. D. Lu, Tuning ionic transport in memristive devices by graphene with engineered nanopores, *ACS Nano* 10(3), 3571 (2016)
42. X. Zhao, J. Ma, X. Xiao, Q. Liu, L. Shao, D. Chen, S. Liu, J. Niu, X. Zhang, Y. Wang, R. Cao, W. Wang, Z. Di, H. Lv, S. Long, and M. Liu, Breaking the current-retention dilemma in cation-based resistive switching devices utilizing graphene with controlled defects, *Adv. Mater.* 30(14), 1705193 (2018)
43. V. K. Sangwan, D. Jariwala, I. S. Kim, K. S. Chen, T. J. Marks, L. J. Lauhon, and M. C. Hersam, Gate-tunable memristive phenomena mediated by grain boundaries in single-layer MoS_2, *Nat. Nanotechnol.* 10(5), 403 (2015)
44. R. Ge, X. Wu, M. Kim, J. Shi, S. Sonde, L. Tao, Y. Zhang, J. C. Lee, and D. Akinwande, Atomristor: Nonvolatile resistance switching in atomic sheets of transition metal dichalcogenides, *Nano Lett.* 18(1), 434 (2018)
45. R. Ge, X. Wu, L. Liang, S. M. Hus, Y. Gu, E. Okogbue, H. Chou, J. Shi, Y. Zhang, S. K. Banerjee, Y. Jung, J. C. Lee, and D. Akinwande, A library of atomically thin 2D materials featuring the conductive-point resistive switching phenomenon, *Adv. Mater.* 33(7), e2007792 (2021)
46. H. Zhao, Z. Dong, H. Tian, D. DiMarzi, M. G. Han, L. Zhang, X. Yan, F. Liu, L. Shen, S. J. Han, S. Cronin, W. Wu, J. Tice, J. Guo, and H. Wang, Atomically thin femtojoule memristive device, *Adv. Mater.* 29(47), 1703232 (2017)
47. Q. Zhao, Z. Xie, Y. P. Peng, K. Wang, H. Wang, X. Li, H. Wang, J. Chen, H. Zhang, and X. Yan, Current status and prospects of memristors based on novel 2D materials, *Mater. Horiz.* 7(6), 1495 (2020)
48. Y. Cao, V. Fatemi, A. Demir, S. Fang, S. L. Tomarken, J. Y. Luo, J. D. Sanchez-Yamagishi, K. Watanabe, T. Taniguchi, E. Kaxiras, R. C. Ashoori, and P. Jarillo-Herrero, Correlated insulator behaviour at half-filling in magic-angle graphene superlattices, *Nature* 556(7699), 80 (2018)
49. J. M. Park, Y. Cao, K. Watanabe, T. Taniguchi, and P. Jarillo-Herrero, Tunable phase boundaries and ultrastrong coupling superconductivity in mirror symmetric magic-angle trilayer graphene, arXiv: 2012.01434 (2020)
50. J. W. Jiang, Graphene versus MoS_2: A short review, *Front. Phys.* 10(3), 287 (2015)
51. R. Wang, X. G. Ren, Z. Yan, L. J. Jiang, W. E. I. Sha, and G. C. Shan, Graphene based functional devices: A short review, *Front. Phys.* 14(1), 13603 (2019)
52. X. M. Huang, L. Z. Liu, S. Zhou, and J. J. Zhao, Physical properties and device applications of graphene oxide, *Front. Phys.* 15(3), 33301 (2020)

53. Q. A. Vu, H. Kim, V. L. Nguyen, U. Y. Won, S. Adhikari, K. Kim, Y. H. Lee, and W. J. Yu, A high-on/off-ratio floating-gate memristor array on a flexible substrate via CVD-grown large-area 2D layer stacking, *Adv. Mater.* 29(44), 1703363 (2017)

54. L. Pósa, M. El Abbassi, P. Makk, B. Sánta, C. Nef, M. Csontos, M. Calame, and A. Halbritter, Multiple physical time scales and dead time rule in few-nanometers sized graphene–SiO_x-graphene memristors, *Nano Lett.* 17(11), 6783 (2017)

55. Y. Ji, S. A. Lee, A. N. Cha, M. Goh, S. Bae, S. Lee, D. I. Son, and T. W. Kim, Resistive switching characteristics of ZnO–graphene quantum dots and their use as an active component of an organic memory cell with one diode-one resistor architecture, *Org. Electron.* 18, 77 (2015)

56. D. I. Son, T. W. Kim, J. H. Shim, J. H. Jung, D. U. Lee, J. M. Lee, W. I. Park, and W. K. Choi, Flexible organic bistable devices based on graphene embedded in an insulating poly(methyl methacrylate) polymer layer, *Nano Lett.* 10(7), 2441 (2010)

57. Y. T. Chan, Y. Fu, L. Yu, F. Y. Wu, H. W. Wang, T. H. Lin, S. H. Chan, M. C. Wu, and J. C. Wang, Compacted self-assembly graphene with hydrogen plasma surface modification for robust artificial electronic synapses of gadolinium oxide memristors, *Adv. Mater. Interfaces* 7(20), 2000860 (2020)

58. T. Berzina, K. Gorshkov, V. Erokhin, V. Nevolin, and Y. A. Chaplygin, Investigation of electrical properties of organic memristors based on thin polyaniline-graphene films, *Russ. Microelectron.* 42(1), 27 (2013)

59. H. He, J. Klinowski, M. Forster, and A. Lerf, A new structural model for graphite oxide, *Chem. Phys. Lett.* 287(1–2), 53 (1998)

60. S. Qin, J. Zhang, D. Fu, D. Xie, Y. Wang, H. Qian, L. Liu, and Z. Yu, A physics/circuit-based switching model for carbon-based resistive memory with sp^2/sp^3 cluster conversion, *Nanoscale* 4(20), 6658 (2012)

61. H. Y. Jeong, J. Y. Kim, J. W. Kim, J. O. Hwang, J. E. Kim, J. Y. Lee, T. H. Yoon, B. J. Cho, S. O. Kim, R. S. Ruoff, and S. Y. Choi, Graphene oxide thin films for flexible nonvolatile memory applications, *Nano Lett.* 10(11), 4381 (2010)

62. F. Zhao, L. Wang, Y. Zhao, L. Qu, and L. Dai, Graphene oxide nanoribbon assembly toward moisture-powered information storage, *Adv. Mater.* 29(3), 1604972 (2017)

63. M. Lübben, S. Wiefels, R. Waser, and I. Valov, Processes and effects of oxygen and moisture in resistively switching TaO_x and HfO_x, *Adv. Electron. Mater.* 4(1), 1700458 (2018)

64. F. Zhuge, B. Hu, C. He, X. Zhou, Z. Liu, and R. W. Li, Mechanism of nonvolatile resistive switching in graphene oxide thin films, *Carbon* 49(12), 3796 (2011)

65. D. P. Sahu, P. Jetty, and S. N. Jammalamadaka, Graphene oxide based synaptic memristor device for neuromorphic computing, *Nanotechnology* 32(15), 155701 (2021)

66. J. Liu, Z. Zeng, X. Cao, G. Lu, L. H. Wang, Q. L. Fan, W. Huang, and H. Zhang, Preparation of MoS_2-polyvinylpyrrolidone nanocomposites for flexible nonvolatile rewritable memory devices with reduced graphene oxide electrodes, *Small* 8(22), 3517 (2012)

67. C. Tan, X. Qi, Z. Liu, F. Zhao, H. Li, X. Huang, L. Shi, B. Zheng, X. Zhang, L. Xie, Z. Tang, W. Huang, and H. Zhang, Self-assembled chiral nanofibers from ultrathin low-dimensional nanomaterials, *J. Am. Chem. Soc.* 137(4), 1565 (2015)

68. J. Yuan and J. Lou, Memristor goes two-dimensional, *Nat. Nanotechnol.* 10(5), 389 (2015)

69. P. Cheng, K. Sun, and Y. H. Hu, Memristive behavior and ideal memristor of 1T phase MoS_2 nanosheets, *Nano Lett.* 16(1), 572 (2016)

70. M. Yoshida, R. Suzuki, Y. Zhang, M. Nakano, and Y. Iwasa, Memristive phase switching in two-dimensional 1T-TaS_2 crystals, *Sci. Adv.* 1(9), e1500606 (2015)

71. S. M. Hus, R. Ge, P. A. Chen, L. Liang, G. E. Donnelly, W. Ko, F. Huang, M. H. Chiang, A. P. Li, and D. Akinwande, Observation of single-defect memristor in an MoS_2 atomic sheet, *Nat. Nanotechnol.* 16, 58 (2020)

72. M. Wang, S. Cai, C. Pan, C. Wang, X. Lian, Y. Zhuo, K. Xu, T. Cao, X. Pan, B. Wang, S. J. Liang, J. J. Yang, P. Wang, and F. Miao, Robust memristors based on layered two-dimensional materials, *Nat. Electron.* 1(2), 130 (2018)

73. H. K. He, R. Yang, W. Zhou, H. M. Huang, J. Xiong, L. Gan, T. Y. Zhai, and X. Guo, Photonic potentiation and electric habituation in ultrathin memristive synapses based on monolayer MoS_2, *Small* 14(15), 1800079 (2018)

74. S. Chen, Z. Lou, D. Chen, and G. Shen, An artificial flexible visual memory system based on an UV-motivated memristor, *Adv. Mater.* 30(7), 1705400 (2018)

75. G. U. Siddiqui, M. M. Rehman, Y. J. Yang, and K. H. Choi, A two-dimensional hexagonal boron nitride/polymer nanocomposite for flexible resistive switching devices, *J. Mater. Chem. C* 5(4), 862 (2017)

76. C. Pan, Y. Ji, N. Xiao, F. Hui, K. Tang, Y. Guo, X. Xie, F. M. Puglisi, L. Larcher, E. Miranda, L. Jiang, Y. Shi, I. Valov, P. C. McIntyre, R. Waser, and M. Lanza, Coexistence of grain-boundaries-assisted bipolar and threshold resistive switching in multilayer hexagonal boron nitride, *Adv. Funct. Mater.* 27(10), 1604811 (2017)

77. X. Wu, R. Ge, P. A. Chen, H. Chou, Z. Zhang, Y. Zhang, S. Banerjee, M. H. Chiang, J. C. Lee, and D. Akinwande, Thinnest nonvolatile memory based on monolayer *h*-BN, *Adv. Mater.* 31(15), 1806790 (2019)

78. S. Chen, M. R. Mahmoodi, Y. Shi, C. Mahata, B. Yuan, X. Liang, C. Wen, F. Hui, D. Akinwande, D. B. Strukov, and M. Lanza, Wafer-scale integration of two-dimensional materials in high-density memristive crossbar arrays for artificial neural networks, *Nat. Electron.* 3(10), 638 (2020)

79. W. Lv, H. Wang, L. Jia, X. Tang, C. Lin, L. Yuwen, L. Wang, W. Huang, and R. Chen, Tunable nonvolatile memory behaviors of PCBM–MoS_2 2D nanocomposites through surface deposition ratio control, *ACS Appl. Mater. Interfaces* 10(7), 6552 (2018)

80. J. C. Wang, Y. T. Chan, W. F. Chen, M. C. Wu, and C. S. Lai, Interface modification of bernal- and rhombohedral-stacked trilayer-graphene/metal electrode on resistive switching of silver electrochemical metallization cells, *ACS Appl. Mater. Interfaces* 9(42), 37031 (2017)
81. X. Zhao, Z. Wang, Y. Xie, H. Xu, J. Zhu, X. Zhang, W. Liu, G. Yang, J. Ma, and Y. Liu, Photocatalytic reduction of graphene oxide-TiO_2 nanocomposites for improving resistive-switching memory behaviors, *Small* 14(29), 1801325 (2018)
82. R. B. Jacobs-Gedrim, M. T. Murphy, F. Yang, N. Jain, M. Shanmugam, E. S. Song, Y. Kandel, P. Hesamaddin, H. Y. Yu, M. P. Anantram, D. B. Janes, and B. Yu, Reversible phase-change behavior in two-dimensional antimony telluride (Sb_2Te_3) nanosheets, *Appl. Phys. Lett.* 112(13), 133101 (2018)
83. P. Saini, M. Singh, J. Thakur, R. Patil, Y. R. Ma, R. P. Tandon, S. P. Singh, and A. K. Mahapatro, Probing the mechanism for bipolar resistive switching in annealed graphene oxide thin films, *ACS Appl. Mater. Interfaces* 10(7), 6521 (2018)
84. X. Sun, Z. Lu, Z. Chen, Y. Wang, J. Shi, M. Washington, and T. M. Lu, Single-crystal graphene-directed van der waals epitaxial resistive switching, *ACS Appl. Mater. Interfaces* 10(7), 6730 (2018)
85. S. I. Oh, J. R. Rani, S. M. Hong, and J. H. Jang, Self-rectifying bipolar resistive switching memory based on an iron oxide and graphene oxide hybrid, *Nanoscale* 9(40), 15314 (2017)
86. Y. Li, S. Long, Q. Liu, H. Lv, and M. Liu, Resistive switching performance improvement via modulating nanoscale conductive filament, involving the application of two-dimensional layered materials, *Small* 13(35), 1604306 (2017)
87. X. Zhao, S. Liu, J. Niu, L. Liao, Q. Liu, X. Xiao, H. Lv, S. Long, W. Banerjee, W. Li, S. Si, and M. Liu, Confining cation injection to enhance CBRAM performance by nanopore graphene layer, *Small* 13(35), 1603948 (2017)
88. R. Shi, X. Wang, Z. Wang, L. Cao, M. Song, X. Huang, J. Liu, and W. Huang, Fully solution-processed transparent nonvolatile and volatile multifunctional memory devices from conductive polymer and graphene oxide, *Adv. Electron. Mater.* 3(8), 1700135 (2017)
89. C. Baeumer, R. Valenta, C. Schmitz, A. Locatelli, T. O. Menteş, S. P. Rogers, A. Sala, N. Raab, S. Nemsak, M. Shim, C. M. Schneider, S. Menzel, R. Waser, and R. Dittmann, Subfilamentary networks cause cycle-to-cycle variability in memristive devices, *ACS Nano* 11(7), 6921 (2017)
90. C. Pan, E. Miranda, M. A. Villena, N. Xiao, X. Jing, X. Xie, T. Wu, F. Hui, Y. Shi, and M. Lanza, Model for multi-filamentary conduction in graphene/hexagonal-boron–nitride/graphene based resistive switching devices, *2D Mater.* 4 (2), 025099 (2017)
91. G. Anoop, V. Panwar, T. Y. Kim, and J. Y. Jo, Resistive switching in ZnO nanorods/graphene oxide hybrid multilayer structures, *Adv. Electron. Mater.* 3(5), 1600418 (2017)
92. P. Zhang, C. Gao, B. Xu, L. Qi, C. Jiang, M. Gao, and D. Xue, Structural phase transition effect on resistive switching behavior of MoS_2-polyvinylpyrrolidone nanocomposites films for flexible memory devices, *Small* 12(15), 2077 (2016)
93. V. K. Nagareddy, M. D. Barnes, F. Zipoli, K. T. Lai, A. M. Alexeev, M. F. Craciun, and C. D. Wright, Multilevel ultrafast flexible nanoscale nonvolatile hybrid graphene oxide–titanium oxide memories, *ACS Nano* 11(3), 3010 (2017)
94. F. Fan, B. Zhang, Y. Cao, and Y. Chen, Solution-processable poly(N-vinylcarbazole)-covalently grafted MoS_2 nanosheets for nonvolatile rewritable memory devices, *Nanoscale* 9(7), 2449 (2017)
95. T. Li, P. Sharma, A. Lipatov, H. Lee, J. W. Lee, M. Y. Zhuravlev, T. R. Paudel, Y. A. Genenko, C. B. Eom, E. Y. Tsymbal, A. Sinitskii, and A. Gruverman, Polarization-mediated modulation of electronic and transport properties of hybrid MoS_2–$BaTiO_3$–$SrRuO_3$ tunnel junctions, *Nano Lett.* 17(2), 922 (2017)
96. C. H. Bok, C. Wu, and T. W. Kim, Operating mechanisms of highly-reproducible write-once-read-many-times memory devices based on graphene quantum dot: poly(methyl silsesquioxane) nanocomposites, *Appl. Phys. Lett.* 110(1), 013301 (2017)
97. A. Rani, D. B. Velusamy, R. H. Kim, K. Chung, F. M. Mota, C. Park, and D. H. Kim, Non-volatile ReRAM devices based on self-assembled multilayers of modified graphene oxide 2D nanosheets, *Small* 12(44), 6167 (2016)
98. G. H. Shin, C.-K. Kim, G. S. Bang, J. Y. Kim, B. C. Jang, B. J. Koo, M. H. Woo, Y. K. Choi, and S. Y. Choi,Multilevel resistive switching nonvolatile memory based on MoS_2 nanosheet-embedded graphene oxide, *2D Mater.* 3(3), 034002 (2016)
99. K. Qian, R. Y. Tay, V. C. Nguyen, J. Wang, G. Cai, T. Chen, E. H. T. Teo, and P. S. Lee, Hexagonal boron nitride thin film for flexible resistive memory applications, *Adv. Funct. Mater.* 26(13), 2176 (2016)
100. C. Hao, F. Wen, J. Xiang, S. Yuan, B. Yang, L. Li, W. Wang, Z. Zeng, L. Wang, Z. Liu, and Y. Tian, Liquid-exfoliated black phosphorous nanosheet thin films for flexible resistive random access memory applications, *Adv. Funct. Mater.* 26(12), 2016 (2016)
101. H. Tian, H. Zhao, X. F. Wang, Q. Y. Xie, H. Y. Chen, M. A. Mohammad, C. Li, W. T. Mi, Z. Bie, C. H. Yeh, Y. Yang, H. S. P. Wong, P. W. Chiu, and T. L. Ren, In situ tuning of switching window in a gate-controlled bilayer graphene-electrode resistive memory device, *Adv. Mater.* 27(47), 7767 (2015)
102. G. Khurana, P. Misra, N. Kumar, and R. S. Katiyar, Tunable power switching in nonvolatile flexible memory devices based on graphene oxide embedded with ZnO nanorods, *J. Phys. Chem. C* 118(37), 21357 (2014)
103. Y. J. Huang and S. C. Lee, Graphene/*h*-BN heterostructures for vertical architecture of RRAM design, *Sci. Rep.* 7, 9679(2017)

104. Y. T. Lee, J. Lee, H. Ju, J. A. Lim, Y. Yi, W. K. Choi, D. K. Hwang, and S. Im, Nonvolatile charge injection memory based on black phosphorous 2D nanosheets for charge trapping and active channel layers, *Adv. Funct. Mater.* 26(31), 5701 (2016)

105. C. Yeon, S. J. Yun, J. Yang, D. H. Youn, and J. W. Lim, Na-cation-assisted exfoliation of MX_2 (M = Mo, W; X = S, Se) nanosheets in an aqueous medium with the aid of a polymeric surfactant for flexible polymer-nanocomposite memory applications, *Small* 14(2), 1702747 (2018)

106. I. Valov and G. Staikov, Nucleation and growth phenomena in nanosized electrochemical systems for resistive switching memories, *J. Solid State Electrochem.* 17(2), 365 (2013)

107. A. Tsurumaki-Fukuchi, R. Nakagawa, M. Arita, and Y. Takahashi, Smooth interfacial scavenging for resistive switching oxide via the formation of highly uniform layers of amorphous TaO_x, *ACS Appl. Mater. Interfaces* 10(6), 5609 (2018)

108. B. Li, Y. Liu, C. Wan, Z. Liu, M. Wang, D. Qi, J. Yu, P. Cai, M. Xiao, Y. Zeng, and X. Chen, Mediating short-term plasticity in an artificial memristive synapse by the orientation of silica mesopores, *Adv. Mater.* 30(16), 1706395 (2018)

109. Q. Wu, H. Wang, Q. Luo, W. Banerjee, J. Cao, X. Zhang, F. Wu, Q. Liu, L. Li, and M. Liu, Full imitation of synaptic metaplasticity based on memristor devices, *Nanoscale* 10(13), 5875 (2018)